https://doi.org/10.48047/AFJBS.6.13.2024.7143-7155

African Journal of Biological Sciences

Journal homepage: http://www.afjbs.com

Research Paper Open Access

FERRIC REDUCING ANTIOXIDANT POWER AND CYTOTOXICITY ACTIVITY AGAINST HUMAN CANCER CELL LINE BY USING CURCUMIN- CHITOSAN NANOPARTICLE

Nabin P Dhal[1], Darshan B Naykude[2], Swathy JS[3], Aditya V Lohokare[4], Praveenkumar D[5], Puniethaa Prabhu[6], Sameer P Sawant[7], Syed Zameer Ahmed Khader[8]

[1,2,4,5,7]M.Tech Biotechnology, Department Of Biotechnology, KS Rangasamy Collage of Technology ,Tiruchengode, India

[6]Professor, Department of Biotechnology, K.S.Rangasamy College of Technology, Tiruchengode, India

[3,8]Associate Professor, Department of Biotechnology, K.S.Rangasamy College of Technology, Tiruchengode, India

[1]dnabinprasad@gmail.com, [2]dbnaykude@gmail.com, [3]swathy@ksrctc.com, [4]aditya28154@gmail.com, [5]dpraveenkumar2201@gmail.com [6]Punithaa@ksrct.ac.in, [6]sameerprakash93@gmail.com, [7]zameerkhader@gmail.com

Volume 6, Issue 13, Aug 2024
Received: 15 June 2024
Accepted: 25 July 2024
Published: 15 Aug 2024
doi: 10.48047/AFJBS.6.13.2024.7143-7155

Abstract - A thorough examination of Chitosan, a direct starch polymer composed of randomly circulated β-(1-4) linked D-glucosamine (a de-acetylated unit) and N-acetyl-D-glucosamine (acetylated units), is presented in this work. Rouget drew it first in 1859, and Hoppe-Seyler gave it an official name in 1894. This cationic polysaccharide has unalienable pharmacological capabilities and is low immunogenic, biocompatible, biodegradable, and effectively accessible. It is also non-lethal. As a result, it is receiving more attention for use in biological and pharmacological applications. Deacetylated chitin, a polysaccharide present in the exoskeleton of shellfish including prawns, lobster and crabs as well as the cell mass of parasites, is what is known as chitosan. After demineralizing the ground exoskeleton with 1% HCl, the exoskeleton is deacetylated with 1⁄2 NaOH to yield chitosan, and finally,After demineralizing the ground exoskeleton with 1% HCl, the exoskeleton is subsequently extracted by dissolving the chitosan in acidic corrosive and reprecipitating it with a pH shift. Chitosan is obtained by deacetylation with 1/2 NaOH. Commercially available CS is 66–95% deacetylated and has a typical atomic weight of between 3800 and 20,000 Daltons. The payback for CS on the amine bunches is approximately 6.5. At neutral pH, it is insoluble, but at acidic pH, it becomes soluble when the chitosan's amino group prorogates and becomes noticeably charged. Through quaternization, the solubility of chitosan in neutral and basic pH can be increased. The atomic weight and degree of organic matter in chitosan have a significant influence on its physicochemical and organic properties. The atomic weight and degree of deacetylation of chitosan have a significant influence on its physicochemical and organic properties. The quantity of protonatable amine groups determines the degree of deacetylation, which in turn determines the polymer's hydrophobicity, solubility, and ability to interact electrostatically with polyanions. The subatomic weight is also very important. Generally speaking, chitosan with lower subatomic weights and deacetylation levels exhibits more notable dissolvability and quicker debasement than its counterparts with higher subatomic weights.

Index Terms - Acetylated unit, Cationic Polysaccharide, Chitosan, De-acetylated unit, Hydrophobicity, Polyanions, Quaternization.

I. INTRODUCTION

Nanotechnology is used in a variety of pharmaceutical-related applications. Even while traditional carriers can generally be utilized to

reduce the number of administration doses and increase delivery efficiency while reducing the unfavourable effects of drug toxicity, injectable nanoparticulate carriers have significant potential applications. To accomplish this goal, monodispersed biodegradable nanospheres were created that could be freeze-dried and quickly redistributed in aqueous solutions without the need for additions. Nanotechnology is used in a variety of pharmaceutical-related applications. Even while traditional carriers can generally be utilized to reduce the number of administration doses and increase delivery efficiency while reducing the unfavourable effects of drug toxicity, injectable nanoparticulate carriers have significant potential applications. To achieve this goal, monodispersed biodegradable nanospheres were produced. To achieve this goal, monodispersed biodegradable nanospheres were created that could be freeze-dried and quickly redispersed in aqueous solutions without the need for additions.

These drug carriers have been used in a variety of pharmaceutical applications. One area of study is the interaction of nanoparticles with immune system components. Nanoparticles can be tailored to avoid immune system identification, or to intentionally diminish or amplify immunological responses. Nanoparticle-mediated immune system stimulation and suppression can be explained by the fact that particle physicochemical properties can influence their interaction with immune cells, resulting in desired immunomodulation while avoiding unwanted immunotoxicity. Furthermore, multiple studies have demonstrated the efficacy of nanoparticles as an antigen delivery mechanism. New breakthroughs in nanotechnology have made it possible to create drug nanoparticles that can be used in a variety of novel ways (Gupta RB et al. 2006).

Although nanoparticles offer many advantages as medication transporter frameworks, there are still many unanswered questions, such as poor oral bioavailability, precariousness in available for use, insufficient tissue conveyance, and toxicity. For example, their small size and large surface area can encourage molecule accumulation, making physical treatment of nanoparticles difficult in fluid and dry structures. The major likes of nanoparticles as a conveyance framework are in controlling molecule calculate, surface properties, and the arrival of pharmacologically dynamic specialists with the aim of achieving the site-particular activity of the medication at the remedially ideal rate and measurements regimen. Although nanoparticles offer many advantages as medication transporter frameworks, there are still many unanswered questions, such as poor oral bioavailability, precariousness in available for use, insufficient tissue conveyance, and toxicity. For example, their small size and large surface area can encourage molecule accumulation, making physical treatment of nanoparticles difficult in fluid and dry structures. The major likes of nanoparticles as a conveyance framework are in controlling molecule calculate, surface properties, and the arrival of pharmacologically dynamic specialists with the aim of achieving the site-particular activity of the medication at the remedially ideal rate and measurements regimen.

Since the 1980s, nanotechnology has received a lot of attention and has been incorporated into a variety of design domains, including mechanical, biomedical, gadget, and space exploration. In particular, nanotechnology has spurred significant advancements in a number of biomedical fields, including tissue engineering, targeted medicine delivery, DNA structure assessment, and controlled medication administration. Nanoparticles are one type of nanomaterial that has advanced this science. In particular, nanoparticle-based therapies have typically proved successful in treating cancer, allergies, diabetes, infections, and inflammation. In science and business, nanotechnology is largely being studied more and more because of its many special uses. Certain industries, like the pharmaceutical industry and restorative development, are extremely passionate about nanotechnology and polymers. Additionally, produced polymers possess. Certain industries, like the pharmaceutical industry and restorative development, are extremely passionate about nanotechnology and polymers. Additionally, produced polymers have shown promise as a tool for nanoscale medication delivery systems, especially when it comes to the oral administration of poorly absorbed prescription medications. Amazing progress has been made in the field of mucoadhesive polymer frameworks in recent years, leading to definitions that extend the duration of medication living arrangements on mucosal films. This, in turn, improves the bioavailability of medications with low oral absorption (Dustagani A et al. 2008).

Cancer Nano therapeutics are quickly evolving and being used to address various drawbacks of traditional drug delivery systems, including nonspecific biodistribution and targeting, a lack of water solubility, poor oral bioavailability, and low therapeutic indices. Nanoparticles have been created with ideal size and surface properties to extend cancer drug circulation time in the bloodstream. They can also preferentially transport their loaded active medications to cancer cells by taking advantage of tumour pathophysiology, such as increased permeability and retention, as well as the tumour microenvironment. In addition to passive targeting, active targeting options employing ligands or antibodies directed at specific tumour targets increase the selectivity of these therapeutic nanoparticles. Drug resistance, which interferes with the efficacy of both molecularly targeted and conventional chemotherapeutic treatments, could also be eliminated or lowered by nanoparticles. P-glycoprotein, one of the key regulators of multidrug resistance, cannot detect nanoparticles in cells, resulting in an increase in intracellular drug concentration. Multifunctional and multiplex nanoparticles are currently being researched and are seen as the next generation of nanoparticles, allowing for personalized and individualized cancer treatment (K Cho et al.2008)

II. MATERIALS AND METHODOLOGY

1. Chemicals and Laboratory equipment's

Acetate of sodium $C_2H_3NaO_2$, Acetic acid glacial CH_3COOH, Hydrochloric acid, Sulfuric acid H_2SO_4, Potassium bromide KBr, Ethanol C_2H_6O, Sodium hydroxide NaOH, N-acetyl glucosamine $C_8H_{15}NO_6$, Solicitor, UV-vis spectrophotometer, Autoclave, Centrifuge, weighing balance, cold room ,pH meter, Hot water bath, etc.

2. Collection of the experimental sample

Shells of Metatarsus magister were collected from the local fish markets of Coimbatore. Figure 1 depicts a schematic illustration of the chitosan synthesis process using crab shells. The shells were washed thoroughly with tap water and then with distilled water to remove impurities and pulverized into powder. Chitosan was extracted in accordance to the method described with some modifications.

3. Preparation of Chitosan

Protein and chitin combine in the exoskeleton tissue to generate a protein-chitin matrix, which is calcified extensively to produce hard shells. Lipids derived from muscle waste and carotenoids, primarily astaxanthin and its esters, may also be present in the waste. The

two main processes in a conventional method for commercially preparing chitin from the exoskeleton (shell) of crustaceans are (A) demineralization by acidic treatment and (b) deproteinization by alkali treatment.

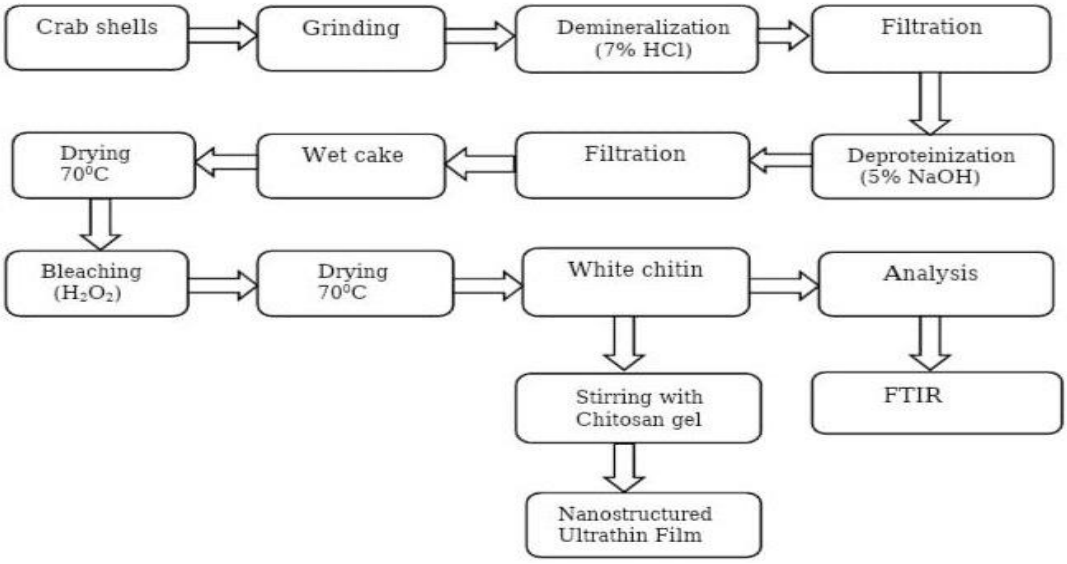

Figure (1) depicts the synthesis of chitosan from crab shells.

1. Demineralization

In Demineralization process, crab shell powder was added slowly to 7% Hydrochloric acid with continuous stirring to avoid effervescence and heated at 60℃ for 2 hours to remove carbonate and phosphate content from the crab shell powder

3.2. Deproteinization

In Deproteinization involves treating the acid hydrolyzed sample with 5% W/V sodium hydroxide to reduce the nitrogen concentration of the protein, subsequently followed by washing to remove any remains of chemical and soluble impurities.

After filtering, the sample was dried for three hours at 70°C in an oven. The dried demineralized, deproteinized and deodorized white sample was obtained. In bleaching step, the dried sample washed with hydrogen peroxide to reduce pigment of chitosan, followed by drying and storing under air tight condition.

3.3. Chitosan Production

Deacetylation of chitin was achieved by reacting chitin with 12.5 M NaOH at a solid/liquid ratio of 1:15 (g/mL). After the reaction mixture was heated to 115 °C and agitated at 250 rpm for four or six hours, it was cooled and maintained frozen at -83 ℃ in an ultra-freezer for twenty-four hours. The resultant chitosan was filtered and rinsed with distilled water to achieve neutral pH.

4. Preparation of chitosan nanoparticles and curcumin loaded chitosan nanoparticles

Chitosan nanoparticles (CNPs) were synthesized by an ionic gelation method as described by Calve et al., 1997. The range of the two compounds (positively charged chitosan and negatively charged sodium tripolyphosphate) in the different ratios was based on pilot experiments, in which only one type of phenomena was observed: an almost clear solution, an opalescent suspension and no aggregates. We were interested in the opalescent solution because of its potential for nanoparticle production.

To put it briefly, 17.5 ml of chitosan solution (1 mg/ml) with and without curcumin (4 mg/ml) was mixed drop wise with an aqueous solution containing 9 ml of sodium tripolyphosphate pentabasic (TPP) (1 mg/ml, pH 5). The chitosan solution was made by dissolving it in 1% acetic acid and using 0.1 M NaOH to get the pH down to 5.0. Even after the particles were left on magnetic stirring for the entire night, nanoparticle production was seen without any aggregation. Curcumin-loaded chitosan nanoparticles (CLCNPs) and CNPs were separated by centrifugation at 8000 rpm for 30 minutes at 4 °C. The pellet was then washed three times with 10% aqueous ethanol. The process was carried out overnight. The pellets were then freeze-dried after being resuspended in 10% aqueous ethanol. This formulation was chosen for curcumin entrapment as well as for additional research and characterization. To put it briefly, 17.5 ml of chitosan solution (1 mg/ml) with and without curcumin (4 mg/ml) was mixed drop wise with an aqueous solution of 9 ml of sodium tripolyphosphate pentabasic (TPP) (1 mg/ml, pH 5). The chitosan solution was made by dissolving it in 1% acetic acid and using 0.1 M NaOH to get the pH down to 5.0. Even after the particles were left on magnetic stirring for the entire night, nanoparticle production was seen without any aggregation. Curcumin-loaded chitosan nanoparticles (CLCNPs) and (CNPs) were separated by centrifugation at 8000 rpm after being stirred for the entire night. Curcumin-loaded chitosan nanoparticles (CLCNPs) and CNPs were separated by centrifugation at 8000 rpm for 30 minutes at 4 °C. The pellet was then washed three times with 10% aqueous ethanol. The process was carried out overnight. The pellets were then freeze-dried after being resuspended in 10% aqueous ethanol. This formulation was chosen for curcumin entrapment as well as for additional research and characterization.

Method of Extraction of Curcumin

4.1. Microwave-assisted extraction of curcumin

For microwave-assisted extraction of curcumin, 0.5 g of turmeric powder was weighed and dissolved in 10 ml acetone and put in a microwave chamber (domestic microwave). Acetone which was used as an extraction solvent has a good dissipation factor which can be heated up to a high extent and dissipate the microwave energy. Extraction was carried out at different microwave operating powers varied between 100-450 W and different irradiation times of 0.5-3 min. The samples were subjected to microwave irradiation in an intermittent way of irradiation-cooling irradiation for an extraction time of up to 3 min because longer irradiation time and higher power

caused boiling of solvent. After that, the solvent was separated through a 0.45 µm filter and evaporated under a vacuum.

5. Phytochemical analysis of curcumin

The curcumin was analyzed for the presence of secondary phytochemicals such as Flavonoids, Phenol, Saponins, Steroids, alkaloids, Fehling's or reducing sugar test, phytosteroids, cardiac glucoside test, Proteins and amino acids.

5.1. Screening for Alkaloids

1 ml of curcumin extract and a few drops of Wagner's reagent, it was sodium iodide and potassium iodide. A prominent brown formation indicates the presence of alkaloids.

5.2. Screening for Phenols

A few drops of 10% Ferric Chloride solution, 1 ml of curcumin extract were added. The creation of the brown colour suggested the existence of phenols.

5.3. Screening for Flavonoids

1 ml of curcumin extract was suspended with a few drops of Sodium Hydroxide solution. The yellow precipitate indicated the presence of Flavonoids.

5.4. Screening for Saponins

1ml of curcumin extract was added with 5 ml of distilled water, the suspension was shaken vigorously and the foam generation indicated the presence of Saponins.

4.5.5. Screening for Steroids

The curcumin extracts were dispersed with 1 ml of Chloroform and 1 ml of acidic anhydride was included after the inclusion of concentrated H_2SO_4 from the sides of the tubes. The formation of the red precipitate ring indicates the presence of steroids.

5.6. Screening for cardiac glucoside

To the extract, a few drops of acidic anhydride were added and shaken well, and then 1 ml of concentrated sulphuric acid was added slowly along the sides of the test tube and allows standing. The formation of a red precipitate indicates the presence of cardiac glucoside.

5.7. Screening for Protein

A few drops of Ninhydrin solution was added to the 1ml extract. The pink colour indicates the presence of proteins.

5.8. Screening for phytosteroids

1ml of the extract few drops of concentrated sulphuric acid was added. The presence of amino acids is indicated by a formation of red colour.

5.9. Screening for tannin

A few drops of 1% Ferric Chloride solution, 1 ml of curcumin extract were added. The brown colour formation indicated the presence of tannin.

5.10. Reducing sugar test

1 ml of curcumin extract and 1 ml of Fehling - A solution and Fehling – B solution. The formation of green or greenish-blue indicates the presence of reducing sugar.

6. UV–visible absorption studies

The Absorbance studies of curcumin loaded chitosan nanoparticles were performed in a UV 1700 spectrophotometer using a 10 mm path length quartz cuvette. The wavelength range in which the spectra were measured was 200–700 mm. The quantity of the curcumin stock solution was increased from 1% to 10%, and to achieve a final concentration of 100%. Each concentration was followed by the recording of the absorption spectra.

7. DPPH radical scavenging activity

Radical scavenging activity was determined according to (Bracaet al., 2001) (44). The stock solution was prepared by dissolving 4 mg DPPH (2, 2, diphenyl-1-picryl hydrazyl) with 100 mL methanol and stored in dark at 20°C until required. Next, add 500 µL of DPPH along with 500 µL of ethanol to a test tube. Different concentrations (10 µL, 20 µL, 30 µL, 40 µL, 50 µL) of CLCNPs added in test tubes and makeup up to 500 µL by adding ethanol. Finally, add DPPH 500 µL to all test tubes. After giving the reaction mixture a good shake, it was allowed to sit at room temperature for 30 minutes in the dark. At 517 nm, the absorbance was measured; a lower absorbance suggested a higher level of free radical scavenging activity.

The following formula was used to calculate the scavenging activity against DPPH:

$$\text{Scavenging activity \%} = \frac{A517\ (\text{sample}) - A517\ (\text{control})}{A517\ (\text{control})} \times 100$$

Where, A517 (control) was the absorbance of the control (DPPH solution without the sample), A517 (sample) was the absorbance of DPPH solution in the presence of the sample (extract/standard).

8. Ferric reducing antioxidant power (FRAP) assay

The antioxidant capacity of samples was estimated according to the procedure described by Benzie and Strain (1996) and as modified by Pulido et al. (2000). FRAP reagent (900 µl), prepared freshly and incubated at 37 ºC, was mixed with 90 µl of distilled water and 30 µl of the test sample, or acetone (for the reagent blank). In a water bath, the test samples and reagent blank were incubated for 30 minutes at 37ºC. The FRAP reagent was composed of 25 ml of pH 3.6 acetate buffer, 2.5 ml of 20 mmol/l $FeCl_3.6H_2O$, and 2.5 ml of 20 mmol/l TPTZ solution in 40 mmol/l HCl (Benzie and Strain, 1996). The calibration curve was prepared using known Fe (II) concentration, $FeSO_4.7H_2O$, which ranges from 100 to 2000 µmol/l. The antioxidant concentration with a ferric-TPTZ reducing capacity equal to 1 mmol/l $FeSO_4.7H_2O$ was designated as the Equivalent Concentration (EC1) parameter. The quantity of antioxidants that increased absorbance in the FRAP experiment to the theoretical absorbance value of a concentration of Fe (II) solution at 1 mmol/l, as estimated by the related regression equation, was computed as EC1.

The Percentage of inhibition = A (control) -A (test) / A control X 100

9. Scanning electron microscopy observation

Scanning Electron Microscopy (SEM) was employed to examine the surface morphology of nanoparticles. A drop of the nanoparticles suspension was placed onto the aluminium stubs located on the surface of the sample stub and dried. The Auto Fine Platinum Coater was then used to coat the stub with a platinum coating prior to imaging. The morphological structure and the diameter of the fibers were analyzed by SEM with an acceleration voltage of 10 kV. To render the electrically conductive samples, they were gold sputter-coated under an argon atmosphere before the experiment.

10. Fourier Transform Infrared (FTIR) spectral study

The FT-IR spectra of curcumin-loaded chitosan nanoparticles were analysed using an FTIR-4600 spectrophotometer to study curcumin entrapment in the polymer matrix. The CLCNPs were crushed with KBr to get the pellets by applying a pressure of 600 kg/cm2. The aforesaid sample's FTIR spectra were obtained in the wavenumber range of 650–4000 cm–1 at a resolution of 2 cm–1. (Kiran et al., 2010) describes how the sample's characteristic peak was measured.

11. X-ray Diffraction (XRD) study

X-ray Diffraction (XRD) was employed to determine the crystal structure of the curcumin-loaded chitosan nanoparticles. To observe the physical nature of curcumin-loaded CPNs, X-ray diffraction (XRD) analysis of the samples were done by (X'Pert-Pro)X-ray Diffractometer using 30 milliamps and 45 kV current with a monochromatic copper anode radiation (λ = 1.54060Å). The scan rate was 0.02° 2θ/s, in the scan range from 2θ = 4 to 60°.

12. In- Vitro Anticancer activity

Cell line

The human Liver Cancer-Hep G2was obtained from National Centre for Cell Science (NCCS), Pune and grown in Eagles Minimum Essential Medium containing 10% fetal bovine serum (FBS). The cells were maintained at 370C, 5% CO2, 95% air and 100% relative humidity. Twice a week, the culture medium was replaced and maintenance cultures were passed through.

Cell treatment procedure

A hemocytometer was used to count the live cells after the monolayer cells were separated using trypsin-ethylene diamine tetra acetic acid (EDTA) to create single cell suspensions. The cells were then diluted with media containing 5% FBS to achieve a final density of 1x105 cells/ml. The 96-well plates were seeded with 100 microliters of cell suspension per well, with a plating density of 10,000 cells/well. The culture conditions were set to 370C, 5% CO2, 95% air, and 100% relative humidity to facilitate cell adhesion. Test sample concentrations were applied in series to the cells after a 24-hour period. Before being diluted with serum-free medium to twice the intended final maximum test concentration, an aliquot of the sample solution was first dissolved in plain dimethyl sulfoxide (DMSO).. Five sample concentrations were obtained by performing four further serial dilutions. The relevant wells already holding 100 µl of medium were filled with aliquots of 100 µl each of these various sample dilutions, resulting in the necessary final sample concentrations. The plates were incubated for a further 48 hours at 370C, 5% CO2, 95% air, and 100% relative humidity after the sample was added. For all concentrations, triplicate of the media without samples was kept as the control.

MTT assay

3[4,5-dimethylthiazol-2-yl]A yellow water soluble tetrazolium salt is called 2,5-diphenyltetrazolium bromide (MTT). The tetrazolium ring is broken by the mitochondrial enzyme succinate-dehydrogenase in live cells, which turns the MTT into an insoluble purple formazan. As a result, the number of viable cells directly correlates with the amount of formazan generated. Each well received 15µl of MTT (5 mg/ml) in phosphate buffered saline (PBS) after 48 hours of incubation, and the wells were then incubated for 4 hours at 370C. After turning off the MTT medium, the formazan crystals were dissolved in 100µl of DMSO, and the absorbance at 570 nm was measured with a microplate reader.

Next, the percentage cell viability was computed in relation to the control using the formula below.

% Cell viability = [A] Test / [A]control x 100

The % cell inhibition was determined using the following formula.

The % Cell Inhibition = (100- Abs)(sample)/Abs (control) x100.

Nonlinear regression graph was plotted between % Cell inhibition and Log concentration and IC50 was determined using Graph Pad Prism software.

III. RESULTS

1. Phytochemical Analysis of Curcumin

The phytochemical components of curcumin are commonly studied using preliminary screening methods. Secondary metabolites were recognised qualitatively as flavonoids, phenol, Saponins, steroid, alkaloids, phytosteroids, cardiac glucoside, proteins, and amino acids.

2. Preparation of Chitosan-Nanoparticle

Metacarcinus magister shells were gathered from Coimbatore's neighbourhood fish shops. After cleaning, they were rinsed with tap water and then distilled water. The shells underwent shade drying, were ground into a powder, and chitosan was extracted using a modified version of the outlined procedure.

Protein and chitin combine in the exoskeleton tissue to generate a protein-chitin matrix, which is calcified extensively to produce hard shells. Lipids derived from muscle waste and carotenoids, primarily astaxanthin and its esters, may also be present in the waste. The two main steps in a traditional commercial preparation process for chitin from crustacean shells (exoskeletons) are (A) deproteinization by alkali treatment and (B) demineralization by acidic treatment at high temperature. Chemical reagents are then used in a bleaching step to produce a colourless product. To remove the carbonate and phosphate content from the crab shell powder, it was demineralized by gently adding it to 7% hydrochloric acid while stirring constantly to prevent effervescence. The mixture was then heated to 60°C for

two hours.

The acid hydrolyzed sample was treated with 5% W/V sodium hydroxide during the deproteinization phase to lower the protein's nitrogen concentration. This was followed by washing to get rid of any remaining chemical and soluble contaminants. After filtering, the sample was dried for three hours at 70°C in an oven. The white sample was dried, deproteinized, deoderized, and demineralized. In the bleaching process, the dried sample is cleaned with hydrogen peroxide to lessen the chitosan's pigment.

Chitosan was created utilising the ionic gelation process. Several amounts of chitosan (1-5 mg) have been added to 1% acetic acid (v/v) and completely mixed through a magnetic stirrer before adding 1% TPP (w/v) dropwise. The solution was then centrifuged at 10,000 rpm for 10 minutes to remove residual TPP, after which the particles were freeze dried..

Figure .2. Crab Shell

Figure.3. Crab Shell Powder.

Figure.4. Chitosan

3. UV analysis of Curcumin loaded chitosan nanoparticles

Ultraviolet-Visible spectra of as-prepared sample in range between 200-800 nm. The plant sample was deposited on clean glass substrate using screen printing technique. The Figure-2 shows optical absorbance spectrum of as prepared film at 100◦C.UV-Vis results shows the presence totally 8 peaks of are 220 nm shows 5.113 absorbance and 250 nm shows 2.383 absorbance, 300 nm and 1.215 absorbance and shows 400 nm weave length shows high degree of 0.697 absorbance and 500,600, 700, 800 nm shows 0.398, 0.285, 0.252 and 0.205 respectively . From this UV results finds the confirmation of functional are present in the plant extract.

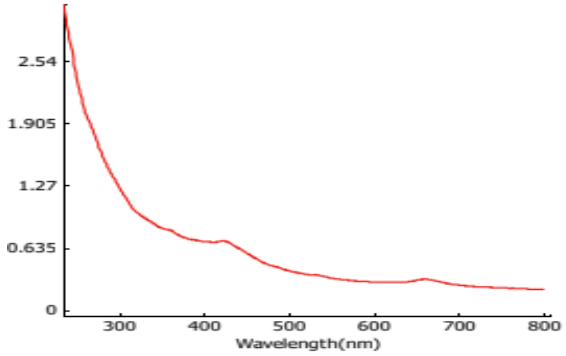

Figure.5. UV profile of Curcumin loaded chitosan nanoparticles.

4. SEM Analysis

The morphology was confirmed by SEM. The scanning electron microscopy picture of chitosan nanoparticles coated with curcumin reveals spherical particles with a 200 nm size range. Nanoparticles should be large enough to avoid rapid leakage into blood capillaries but small enough to avoid capture by macrophages stuck in the reticulo-endothelial system when delivering drugs via nanoparticles.

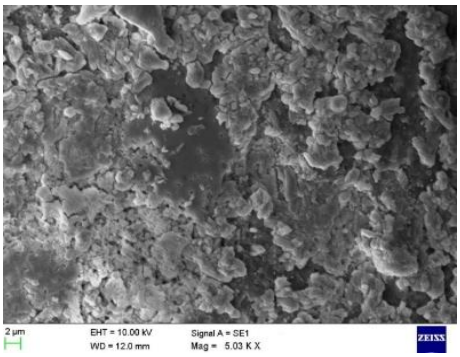

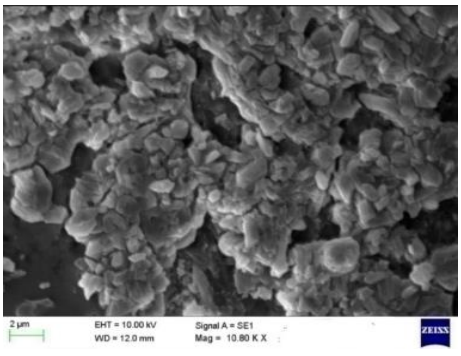

Figure.6. SEM image of curcumin loaded chitosan nanoparticles.

5. FTIR spectroscopy analysis

Further, to confirm the loading of drug in the curcumin loaded chitosan nanoparticles formulation, FTIR analysis was conducted. Fig.

4 shows the FT-IR spectra of curcumin loaded chitosan nanoparticles. The IR spectrum of Curcumin demonstrated stretching vibrations due to phenolic hydroxyl groups at 3200–3500 cm-1, In chitosan, a peak at 1635 cm-1 was observed, and this corresponds to amide I bending vibration. In the CsNPs spectrum, the wave number shifted from 1640 to 870cm-1. The vibrational mode of amide C-O stretching was observed at 1635, cm-1. The spectra were also compared with the standard chitosan and correlations were observed in the spectra are shown in (Figure 7).In the spectra of CLCsNPs, a peak at 689 cm-1 was observed, which corresponds to amino deformation, and a change in the peak at 555 cm-1 corresponds to the -keto group of the curcumin. The FT-IR data reveal that the NPs were produced as a result of an interaction between TPP's phospho groups and chitosan's amino groups. The FT-IR data reveal that the NPs were produced as a result of an interaction between TPP's phospho groups and chitosan's amino groups. There was an interaction between the -keto group of curcumin and the amine group of chitosan that resulted in drug loading.

6. XRD study

Multiple peaks in the 2 range of 15–35° are visible in the broad XRD patterns of CLCsNPs, curcumin, and chitosan, suggesting the crystalline form of the component. The CLCsNPs exhibited strong reflections around 22.81o, 26.21o, 27.96o, and 28.66o. The XRD plots for curcumin-loaded CPNs are presented. This result indicates that curcumin encapsulated in NPs is in the solid-state solubilized form in the polymeric matrix. This disordered-crystalline phase of curcumin inside the polymeric matrix helps in the sustained release of the drug from the nanoparticles.

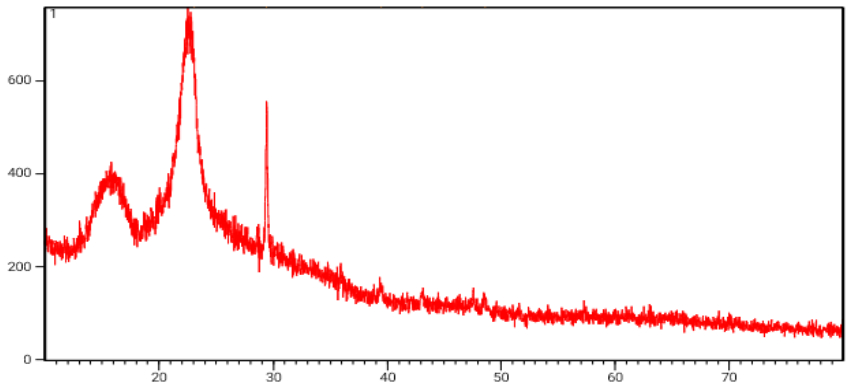

Figure.7. XRD pattern of curcumin loaded CsNPs.

7. Antioxidant Activity

7.1. DPPH Assay

When an antioxidant on the interface with DPPH radical transfers hydrogen or electron atoms to DPPH, the DPPH assay is the radical scavenging of stable 2, 2-diphenyl picryl hydrazyl at room temperature. When DPPH comes into touch with an antioxidant, it is reduced by surrendering its free electron.

Thus, the greater the degree of decolourization, the greater the scavenging activity of the compound. The reducing capacity of DPPH radicals is calculated by the decrease in their absorbance at 517 nm induced by antioxidants. DPPH is a stable free radical that takes an electron or hydrogen radicals to transform into a stable diamagnetic molecule. Therefore, DPPH is usually used as a substance to evaluate antioxidant activity.

The percentage of DPPH radical scavenging activity of the prepared samples is presented as a tabulation and graph (Table 2) and Figure (09)

Table 2: Percentage Of DPPH Inhibition In Curcumin Loaded Chitosan Nano-Particle.

Concentration	Sample	Percentage of inhibition Nanoparticles	Standard (Ascorbic acid)
S-1	10 µl	25. 53 %	15 %
S-2	20 µl	33.42 %	38 %
S-3	30 µl	54.92 %	56 %
S-4	40 µl	69.01 %	73 %
S-5	50 µl	78.02 %	86 %

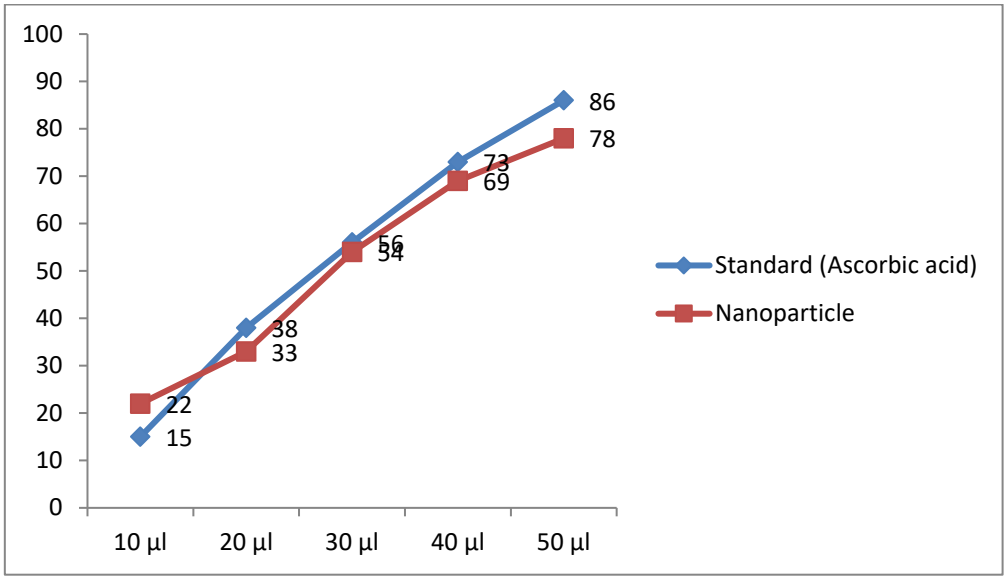

Figure.8.Antioxidant Activity Of Curcumin Loaded Chitosan Nanoparticles.

7.2 Ferric reducing antioxidant power (FRAP) assay

The FRAP assay converts ferric-tripyridyltriazine (FeIII-TPTZ) into ferrous-tripyridyltriazine (FeII-TPTZ), a blue product, in the presence of antioxidants in the samples (Benzie and Strain 1996). "The antioxidant capacity of synthesised nanoparticles varies depending on this material's ability to decrease ferric to ferrous ions." was also measured by adding the FRAP reagent to a variety of Fe2+ solutions with known concentrations, yielding a standard curve.

The FRAP values of curcumin-loaded chitosan nanoparticles are shown in Table 3. The graph shows the progressive decrease in peak height

Table.3.Percentage Of FRAB Inhibition In Curcumin Loaded Chitosan Nano-Particle.

Sr.NO	Concentration	FRAP Ascorbic Acid Standard	Percentage Of Inhibition Nanoparticles
S-1	10 µl	33	22.51
S-2	20 µl	44	32.77
S-3	30 µl	52	48.00
S-4	40 µl	71	71.74
S-5	50 µl	83	84.01

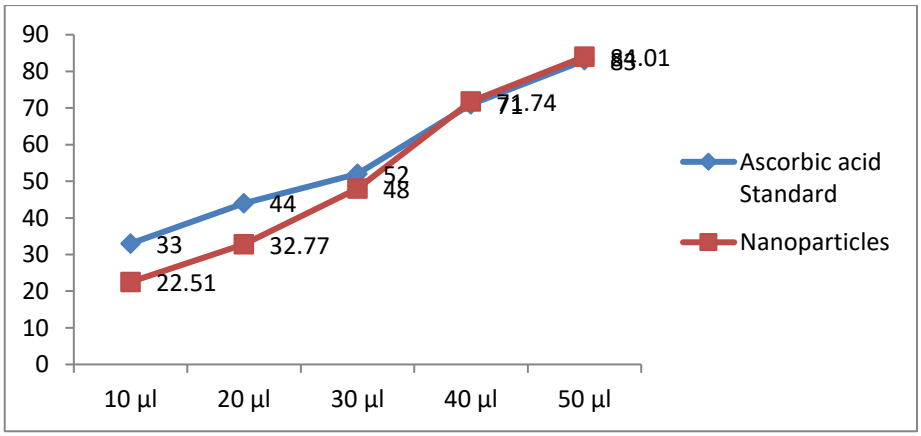

Figure.9. Ferric Reducing Activity Of Curcumin Loaded Chitosan Nanoparticle

5.8. Antibacterial Activities of *Chitosan- Curcumin* Nanoparticles:

Table:4 Anti-bacterial Activities of *Chitosan- Curcumin* Nanoparticles Against *E.Coli*

Sr. No	Concentration	Ring Measurement
1.	Std	1 cm
2.	25µl	1.3cm

3.	50µl	1.5 cm
4.	75µl	1.9cm
5.	100µl	2.0cm

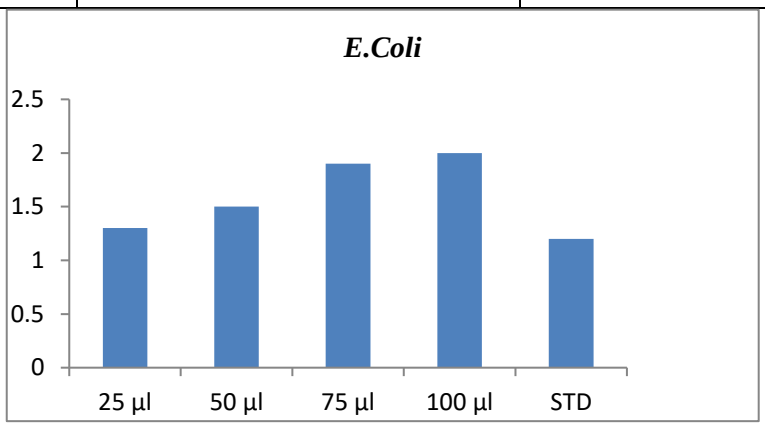

Figure.10. *Chitosan- Curcumin* Nanoparticles Against *E.Coli*

Table.5.Anti-Bacterial Activities Of *Chitosan- Curcumin* Nanoparticles Against *Staphylococcus Aureus*

Sr.NO	Concentration	Ring measurement
1.	Std	1.3cm
2.	25µl	1cm
3.	50µl	1.2cm
4.	75µl	1.5cm
5.	100µl	1.7cm

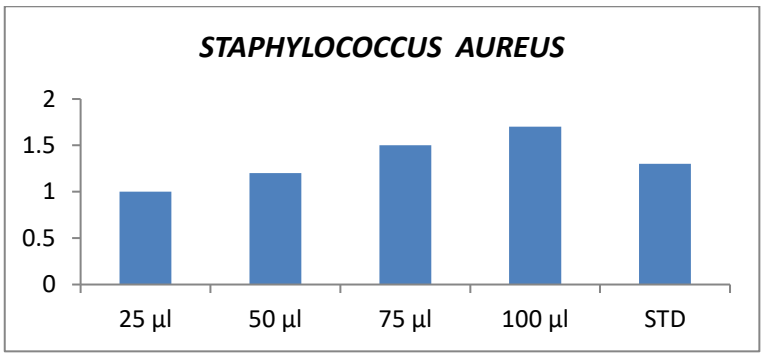

Figure.11. *Chitosan- Curcumin* Nanoparticles Against *Staphylococcus aureus*

Table.6.Anti-bacterial Activities of *Chitosan- Curcumin* Nanoparticles Against *staphylococcus epidermis:*

Sr.NO	Concentration	Ring measurement
1.	Std	2.3cm
2.	25µl	1.7cm
3.	50µl	1.8cm
4.	75µl	2.0cm
5.	100µl	2.2cm

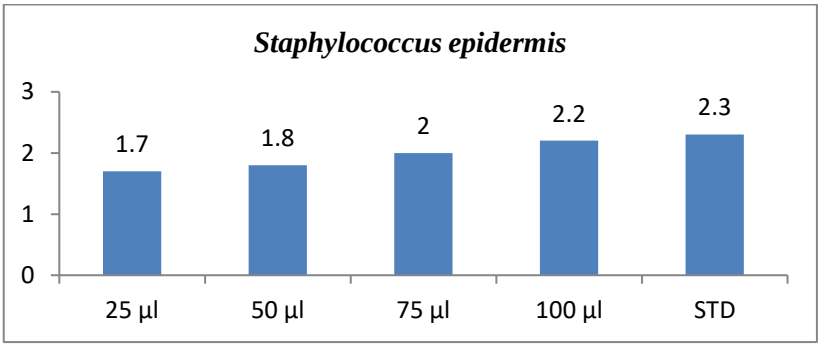

Figure.12.*Chitosan- Curcumin* Nanoparticles Against *Staphylococcus epidermis*

Table.8.Anti-bacterial Activities of *Chitosan- Curcumin* Nanoparticles Against *Streptococusmutans*

Sr.No	Concentration	Ring Measurement
1.	Std	2.9cm
2.	25µl	2.5cm
3.	50µl	2.7cm
4.	75µl	3.0cm
5.	100µl	3.2cm

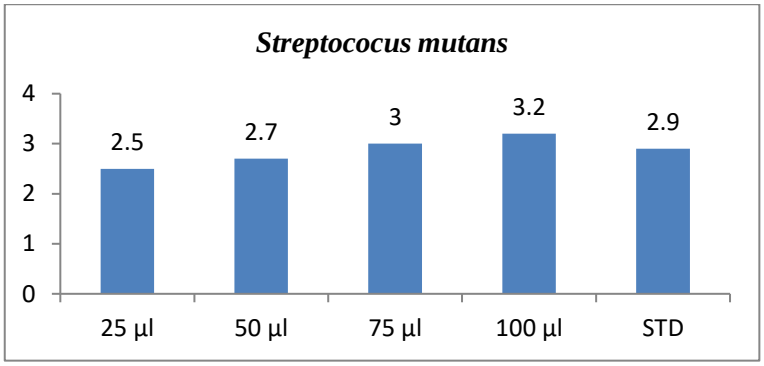

Figure.13.*Chitosan- Curcumin* Nanoparticles Against *Streptococcus mutants*

Table.9. Anti-bacterial Activities of *Chitosan- Curcumin* Nanoparticles Against *Protease vulgaris*

S.No	Concentration	Ring Measurement
1.	Std	2.1cm
2.	25µl	1.5cm
3.	50µl	2.0cm
4.	75µl	2.3cm
5.	100µl	2.4cm

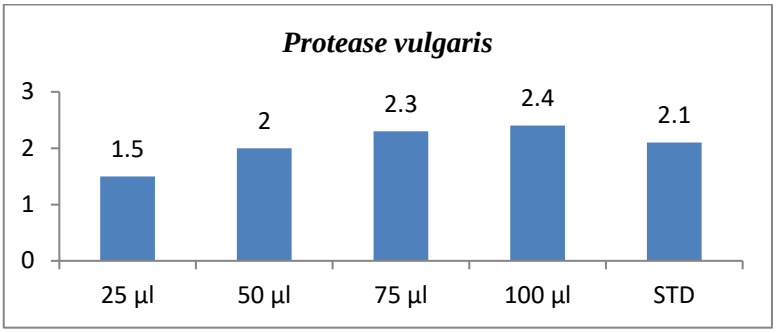

Figure.14.*Chitosan- Curcumin* Nanoparticles Against *Protease vulgaris*

5.9. In-vitro Anticancer activity of curcumin loaded chitosan nanoparticle

Anticancer activity against the Hep-G2 cell line was assessed in vitro at various doses. The anticancer activity of CLCsNPs nanoparticles was tested at various concentrations, including 18.75 µg, 37.5 µg, 75 µg, 150 µg, and 300 µg. CLCsNPs nanoparticles' anticancer efficacy against HepG2 rose as their concentration grew. The anticancer effect of CLCsNPs nanoparticles on HepG-2 cell lines was tested, and the results were promising. The results reveal that there is good cytotoxic effect against cancer cells (Figure 16). CLCsNPs nanoparticles perform well against Hep-G2, with optimal results at 300 µg, 75 µg, and 150 µg. Cell inhibition was lowest at doses of 18.75 µg and 37.5 µg.

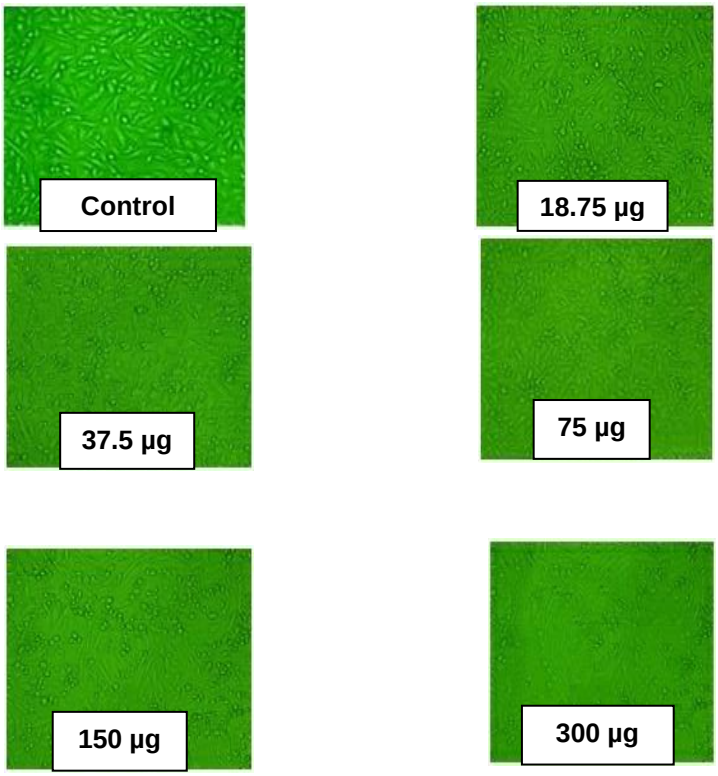

Figure.15.Microscopic images of (HepG2) cell lines after incubation with CLCsNPs

Table 10: Percentage of cell inhibition of CLCsNPs

Conc (µg/Ml)	**% Cell Inhibition**	**Ic 50 174.29**	**µg/Ml**
18.75	8.432709		
37.5	19.3356	**R^2**	**0.996**
75	31.13288		
150	46.50767		
300	58.34753		

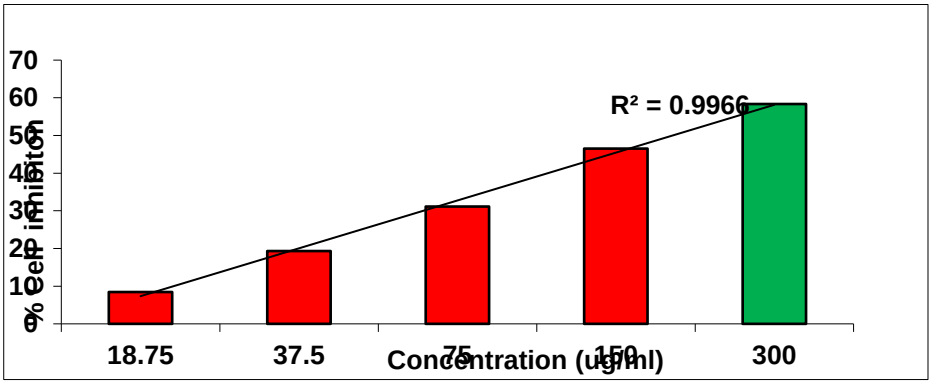

Figure.16. Cell Inhibition Of CLCsNPs Against Liver Cancer (Hepg2) Cell Lines

IV. REFERENCES

[1]Gupta RB, Kompella UB, "Fundamentals of drug nanoparticles", Nanoparticle Technology for Drug Delivery, vol.1, pp. 1-18,New York: Taylor & Francis group; 2006.
[2]Bhattarai N, Ramay HR, Chou SH, Zhang M. "Chitosan and lactic acid-grafted chitosan nanoparticles as carriers for prolonged drug delivery" Int J Nanomedicine. 2006;1(2):181-7.
[3]Dustgani A, Farahani EV, Imani M. "Preparation of chitosan nanoparticles loaded by dexamethasone sodium phosphate" Ir J Pharm Sci. 2008;4(2):111-4.
[4]Gref R, Minamitake Y, Peracchia MT, Trubetskoy V, Torchilin VP, Langer R. Biodegradable long– circulating polymeric nanospherese. Science. 1994; 263(5153):1600-3.
[5]Zolnik BS, González-Fernandez A, Sadrieh N, Dobrovolskaia MA. Nanoparticles and the immune system. Endocrinology. 2010;151(2):458-65.
[6]Sayin B, Somavarapu S, Li XW, Thanou M, Sesardic D, Alpar HO.2008. Mono-N-carboxymethyl chitosan (MCC) and N-trimethyl chitosan (TMC) nanoparticles for non-invasive vaccine delivery. Int J Pharm. 2008; 363(1-2):139-48.
[7]Waghmare A, Deopurkar RL, Salvi N, Khadilkar M, Kalolikar M, Gade SK. Comparison of Montanide adjuvants, IMS 3012 (Nanoparticle), ISA206 and ISA35 (Emulsion based) along with incomplete Freund's adjuvant for hyperimmunization of equines used for production of polyvalent snake antivenom. Vaccine. 2009;27(7):1067-72.
[8]Jain KK. Nanopharmaceuticals. In: The handbook of nanomedicine. Basel, Switzerland: Humana Press; 2008. p. 119-60.
[9]Bravo-Osuna I, Vauthier C, Chacun H, Ponchel G (2008) Eur J Pharm Biopharm., 2008; 69(2): 436.
[10]Bernkop-Schnєurch A, Guggi D, Pinter Y (2004) J Control Release., 2004; 94: 177
[11]AboubakarM, Couvreur P, Pinto AlphandaryH,Gouriton B, Lacour B, Farinotti R, Puisieux F, Vauthier C (2000) Drug Dev Res., 2000; 49: 109.
[12]Panyam, J.; Labhasetwar, V. Biodegradable nanoparticles for drug and gene delivery to cells and tissue. Adv. Drug Deliv. Rev., 2003: 55: 329– 347.
[13]Kataoka, K.; Harada, A.; Nagasaki, Y. Block copolymer micelles for drug delivery: Design, characterization and biological significance. Adv. Drug Deliv. Rev., 2012; 64: 37–48.
[14]Shi, J.; Votruba, A.R.; Farokhzad, O.C.; Langer, R. Nanotechnology in drug delivery and tissue engineering: From discovery to applications. Nano. Lett, 2010; 10: 3223–3230.
[15]Mironov, V.; Kasyanov, V.; Markwald, R.R. Nanotechnology in vascular tissue engineering: from nanoscaffolding towards rapid vessel biofabrication. Trends Biotechnol., 2008; 26: 338– 344.
[16]Koo, O.M.; Rubinstein, I.; Onyuksel, H. Role of nanotechnology in targeted drug delivery and imaging: a concise review. Nanomed. Nanotechnol. Biol. Med., 2005; 1: 193–212.
[17]Hansma, H.G. Surface biology of DNA by atomic force microscopy. Annu. Rev. Phys. Chem., 2001; 52: 71–92.
[18]Brigger, I.; Dubernet, C.; Couvreur, P. Nanoparticles in cancer therapy and diagnosis. Adv. Drug Deliv. Rev., 2012; 64: 24–36.
[19]Basarkar, A.; Singh, J. Poly (lactide-coglycolide)-polymethacrylate nanoparticles for intramuscular delivery of plasmid encoding interleukin-10 to prevent autoimmune diabetes in mice. Pharm. Res., 2009; 26: 72–81.
[20]Roy, K.; Mao, H.-Q.; Huang, S.K.; Leong, K.W. Oral gene delivery with chitosan-DNA nanoparticles generates immunologic protection in a murine model of peanut allergy. Nat. Med., 1999; 5: 387–391.
[21]Furno, F.; Morley, K.S.; Wong, B.; Sharp, B.L.; Arnold, P.L.; Howdle, S.M.; Bayston, R.; Brown, P.D.; Winship, P.D.; Reid, H.J. Silver nanoparticles and polymeric medical devices: a new approach to prevention of infection? J. Antimicrob. Chemother., 2004; 54: 1019–1024.
[22]Wilson, D.S.; Dalmasso, G.; Wang, L.; Sitaraman, S.V.; Merlin, D.; Murthy, N. Orally delivered thioketal nanoparticles loaded with TNFα–siRNA target inflammation and inhibit gene expression in the intestines. Nat. Mater., 2010; 9: 923–928.
[23]Couvreur P, Vauthier C (2006) Pharm Res., 2006; 23(7): 1417.
[24]Rawat M, Singh D, Saraf S, Saraf (2006) Biol Pharm Bull., 2006; 29(9): 1790.
[25]Shweta Dwivedi, AlokMahor and DilipChanchal, chitosan nanoparticles; world journal of pharmacy and pharmaceutical science; Volume 5, Issue 1, 433-439
[26]Patel, M.P., Patel, R.R., and Patel, J.K. 2010. Chitosan Mediated Targeted Drug Delivery System: A Review. J. Pharm. Pharma. Sci., 13:536 – 557.
[27]Jie, J., Wu, W.Z., Zhong, Z.R., Guang, X.T.X., Shu, L.Z., and Wang, L. 2011 Recent Advances of Chitosan Nanoparticles. Int. J.

Nanomedicine. 6:765–774.
[28]Ambore Sandeep* , KanthaleSangameshwar, GavitMukesh, RathodChandrakant, DhadweAvinash
[29]Balmayor E R, Barana E T, Azevedoa H S, Reisa R L, Injectable biodegradable starch/chitosan delivery system for the sustained release of gentamicin to treat bone infections. Carbohydrate polymer 2011 87, 32-39.
[30]Illum L. Chitosan and its use as a pharmaceutical excipient. Pharmaceutical Research, 1998 15(9), 1326–1331.
[31]Illum L, Farraj N F, Davis S S. Chitosan as a novel nasal delivery system for peptide drugs Pharm. Res. 1994, 11:1186–1189.
[32]lChandy T, Mooradian D L, Rao G H R, Chitosan polyethylene glycol alginate microcapsules for oral delivery of hirudin. Journal of Applied Polymer Science, 1998 70(11), 2143–2153.
[33]Agnihotri S. A., Mallikarjuna N. N., &Aminabhavi T. M.,Recent advances on chitosan-based micro- and nanoparticles in drug delivery. Journal of Controlled Release 2004, 100(1), 5–28.
[34]Lin Y. H., Mi F. L, Chen C. T., Chang W. C., Peng S. F., Liang H. F., and Sung H. W.. Preparation and characterization of nanoparticles shelled with chitosan for oral insulin delivery Biomacromolecules 2007, 8:146–152
[35]Cheng M., Deng J., Yang F., Gong Y., Zhao N, & Zhang X. Study on physical properties and nerve cell affinity of composite films from chitosan and gelatin solutions. Biomaterials 2003, 24, 2871–2880.